

A mobilized three-phase absorption thermal energy storage system for district heating and cooling supply

Yao Lin^{1,2}, Fu Xiao^{1,2*}, Shengwei Wang^{1,2}

1 Department of Building Environment and Energy Engineering, The Hong Kong Polytechnic University, Kowloon, Hong Kong

2 Research Institute for Smart Energy, The Hong Kong Polytechnic University, Kowloon, Hong Kong

(*Corresponding Author: linda.xiao@polyu.edu.hk)

ABSTRACT

Mobilized thermal energy storage (M-TES) system can balance the spatial mismatch between the waste heat source and the end-user side. In this study, an experimental test rig has been built to study the dynamic discharging characteristics and the storage performance of a three-phase absorption thermal energy storage (ATES) system. The test rig consists of an electric chiller, electric heaters, a control cabinet, plate heat exchangers and detachable storage tanks for mobilized applications. LiCl solution is chosen as a working fluid for its high energy storage density (ESD). The performances of the proposed storage system under three application scenarios, namely cooling, heating and combined cooling and heating were investigated. The experimental results show that the proposed storage system can achieve the ESD for 484~598 (kJ/kg solution) under different working conditions. The test results verify the potential mobilized application of three-phase ATES in district heating and cooling systems.

Keywords: absorption thermal energy storage, three-phase, mobilized, energy storage density

NONMENCLATURE

Abbreviations

M-TES	Mobilized thermal energy storage
ESD	Energy storage density
ATES	Absorption thermal energy storage
EG	Ethylene Glycol
M	Mass (kg)
m	Mass flow rate (m/s)
T	Temperature (°C)
C _p	Specific heat capacity
H	Enthalpy

X	Concentration
L	Liquid level
<i>Symbols</i>	
dis	Discharging
eva	Evaporator
abs	Absorber
s	Solution
w	Water
v	Vapor
in	Inlet
out	Outlet
h	Het
c	Cold
τ	Time

1. INTRODUCTION

Heating and cooling have consumed around 50% of global energy, which contributes to around 40% of global energy-related carbon emissions [1]. Residential sector and industrial sector are two primary energy consumers around the world. Residential sector consumes around 30% of the world's energy, most of which is consumed by its heating, cooling and ventilation systems [2]. Industrial sector shares another 43% of the total heating amount [3], with up to 33% of it ultimately being directly rejected into the environment as waste heat without further exploitation and utilization [4]. A large proportion of the waste heat has a temperature below 100°C, which limits its application due to its low exergy [5].

District heating and cooling system is considered as a key technology to reduce energy consumption and carbon emission for residential sector [6]. A district heating and cooling system owns chillers and a central heat source plant can provide cooling and heating for a group of adjacent buildings. The produced cold water

and steam (or hot water) are supplied to various buildings through regional pipelines within the district. Since the energy level of low-temperature waste heat is close to the temperature requirement of domestic heating and hot water supply, efforts have been made to the utilization of low-temperature waste heat [7]. Absorption heat pumps, which can be driven by low-temperature waste heat, are widely adopted and have shown promising applications [8, 9].

Despite the huge potential of integrating waste heat recovery with district heating and cooling systems, there exist several challenges. For example, in remote areas, constructing long-distance pipelines between the waste heat source and the end-user side is often costly and inefficient [10]. Besides, the fluctuation and intermittency of waste heat sources also need special concern.

To address these issues, mobilized thermal energy storage (M-TES) has been proposed. The primary goal of M-TES is to develop mobilized thermal energy storage devices that can transport the stored heat to the end-user side [11]. Currently, the storage materials used in M-TES can be grouped into sensible heat storage materials, latent heat storage materials and sorption heat storage materials based on their working principles [12]. Among them, sorption heat storage materials have the highest energy storage density (ESD). They are also characterized by negligible heat loss during transportation, making them promising storage materials in M-TES devices. Typically, as one of the sorption thermal energy storage technologies, absorption thermal energy storage (ATES) uses the same working fluids (i.e. aqueous alkali halide salt solution) with absorption heat pumps. It also has the potential to provide heating and cooling simultaneously. Therefore, ATES can be easily integrated with absorption heat pumps and district heating and cooling systems. Moreover, if a crystallized salt solution is used as the working fluid, the ESD of ATES can be further enhanced. Allowing the presence of crystals during the operation of ATES is called three-phase ATES [13]. The three phases include a liquid phase (the aqueous alkali halide salt solution), a gas phase (the water vapor) and a solid phase (the alkali halide salt crystals) [14]. However, few existing studies have experimentally investigated the energy performance of three-phase ATES.

In this study, a three-phase ATES experimental test rig was established, which can be used as a mobilized TES device. The experiments were conducted under three working conditions, namely cooling, heating and combined cooling and heating. The dynamic discharging

characteristics under different working conditions were studied to characterize its performance. The ESD was calculated and compared based on the experimental data.

2. EXPERIMENTAL METHODS AND PERFORMANCE INDICES

2.1 Working principle and working fluids

The working principle of three-phase ATES can be divided into three processes, charging process, storage process and discharging process. In the charging process, the dilute solution enters the generator and is charged into rich solution by external heat source. The solution's temperature increases and generates water vapor. The generated vapor is transported and condensed into water in the condenser. The condensed water is collected and stored in the water tank. During the storage process, the rich solution and water are stored separately in the storage tanks. The temperatures of solution gradually drop to ambient and crystals form in the solution. In the storage process, no internal heat and mass transfer occurs between the solution and refrigerant water. During the discharging process, the stored water evaporates in the evaporator under high vacuum degree and produces cooling effect. The water vapor is then transported and absorbed by the rich solution, which, as a result, produces heating effect. The crystals dissolve and the rich solution becomes weak solution.

In this study, LiCl solution is selected as the working fluid due to its potential highest ESD among commonly used water-based working fluids, LiCl solution, LiBr solution and CaCl₂ solution [15]. Ethylene glycol is chosen as an additive based on the analysis of our previous work [13]. The mass ratio of LiCl solution: EG is 100:5.

2.2 Experimental test rig and components

An experiment test rig was established to study the dynamic process of charging and discharging characteristics of absorption TES using novel working fluids. Fig.1 shows the schematic of the test rig. The test rig consists of 5 main parts, namely the heat exchangers, solution and water tanks, thermostatic waterbaths, chiller and sensors. Two heat exchangers are the key components of the test rig. The one used for solution generation during the charging process and water absorption during discharging process is called "Generator/Absorber", while the other one used for vapor condensation during charging process and water evaporation during discharging process is called

“Condenser/Evaporator”. The two heat exchangers are connected by a vapor pipe, facilitating the transportation of vapor from the generator to the condenser during the charging process and in reverse during the discharging process. Below the two heat exchangers are two storage tanks, a solution tank and a refrigerant water tank. The solution tank is detachable for mobilized application. The solution tank has a filter inside to prevent crystals from entering the pipes and pumps. Two thermostatic waterbaths, one on solution side and the other one on the water side, are used to provide heat transfer fluids to two plate heat exchangers. The temperatures of both thermostatic waterbaths are controlled and maintained by electric heaters and a chiller.

2.3 Experimental conditions

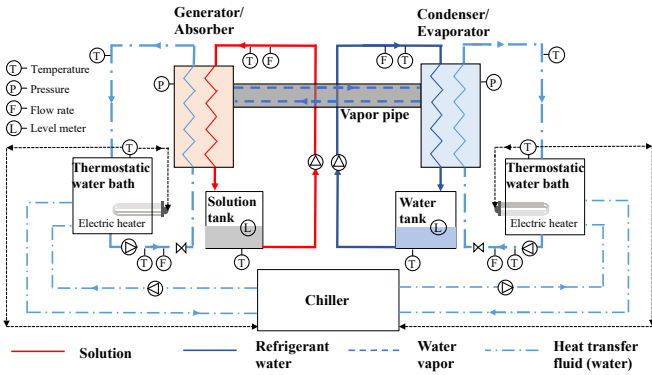


Fig. 1 Schematic of the test rig

In this study, experiments are conducted under different experimental conditions considering its real application scenarios in district heating and cooling supply. Table 1 shows the experimental conditions of discharging tests. Three typical working conditions (i.e. heating, combined heating and cooling, cooling) with different discharging temperatures are selected. Before each discharging experiment begins, the solution was a partially crystallized solution with an initial concentration around 52.5%.

Table 1. Experimental conditions

Discharging	Discharging temperature (°C)	Evaporation temperature (°C)
Heating	50	30
Combined heating and cooling	20 and 40	23
Cooling	12	15

2.4 Thermodynamic correlations and performance indices

The enthalpy of the working fluid is calculated using correlations provided by Chaudhari and Patil [16]. The specific heat capacity of the solution is calculated using the correlations provided by Conde [17]. In the discharging process, heating output ($q_{dis,h}$) and cooling output ($q_{dis,c}$) can be achieved at absorber and evaporator simultaneously. The calculation of heating output rate and cooling output rate are shown in Eq.(1-6). Therefore, the ESD can be specified into heat storage density (ESD_h) and cold storage density (ESD_c), as shown in Eq.(6-7).

$$q_{dis,c} = q_{eva} = c_{p,w} m_{w,eva} (T_{w,eva,out} - T_{w,eva,in}) \quad (1)$$

$$q_{dis,h} = q_{dis,w} = c_{p,w} m_{w,abs} (T_{w,abs,out} - T_{w,abs,in}) \quad (2)$$

$$m_v = \frac{dM_w(\tau)}{d\tau} \quad (3)$$

$$M_w(\tau) = f(L) \quad (4)$$

$$Q_{dis} = \int q_{dis} dt \quad (5)$$

$$ESD_h = \frac{Q_{dis,h}}{M_s} \quad (6)$$

$$ESD_c = \frac{Q_{eva,c}}{M_s} \quad (7)$$

3. RESULT AND DISCUSSIONS

3.1 Discharging characteristics of heating conditions

Fig.2 shows the variation of temperatures, including the temperatures of solution, refrigerant water and heat exchange fluids at the inlet and outlet of the absorber. For heating application, the solution temperature gradually increases at the beginning 60 mins of the discharging process. The discharging heat during this process is mainly used for the solution's temperature rise. After 60 mins, the solution temperature is kept above 50°C. The total discharging process lasts for about 4 hours.

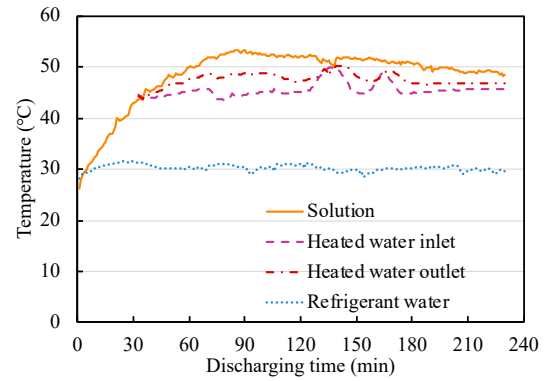


Fig. 2 Variation of the temperatures for heating

Fig.3 shows the variation in concentration and heat output rate during the discharging process. It can be found that the discharging rate drops along the

discharging process, which is caused by the decrease of solution's concentration.

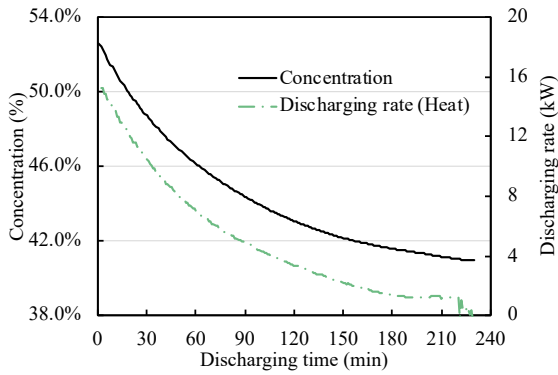


Fig. 3 Variation of the concentration and discharging rate for heating

3.2 Discharging characteristics of combined heating and cooling condition

Fig.4 and Fig.5 show the discharging characteristics for combined heating and cooling. Similarly, the solution temperature increases at the first 60 mins. Compared with the heating condition, lower evaporation temperature brings lower absorption temperature and lower heat and cold discharging rate.

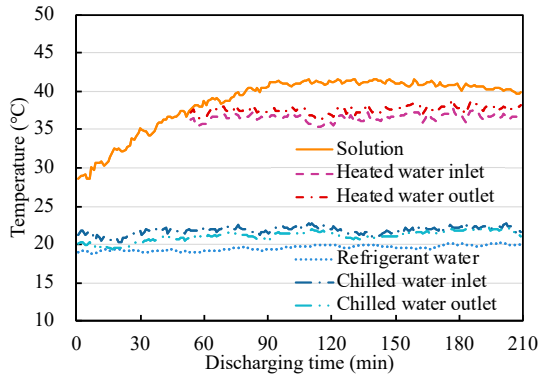


Fig. 4 Variation of the temperatures for combined heating and cooling

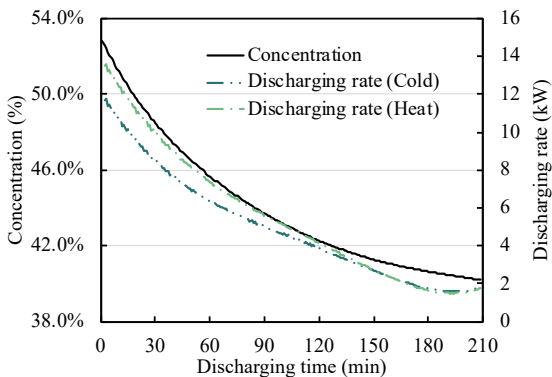


Fig. 5 Variation of the concentration and discharging rate for combined heating and cooling

3.3 Discharging characteristics of cooling condition

Fig.6 and Fig.7 exhibit the discharging characteristics for cooling. Since there is no heating requirement, the solution's temperature is kept at a lower level. The evaporation temperature is around 10°C. The concentration after discharging is still around 41%. However, the lowest evaporation temperature leads to the lowest cold discharging rate and longest discharging time to reach the same concentration after discharging.

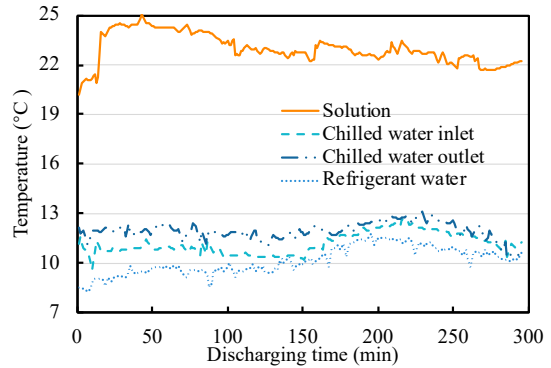


Fig. 6 Variation of the temperatures for cooling

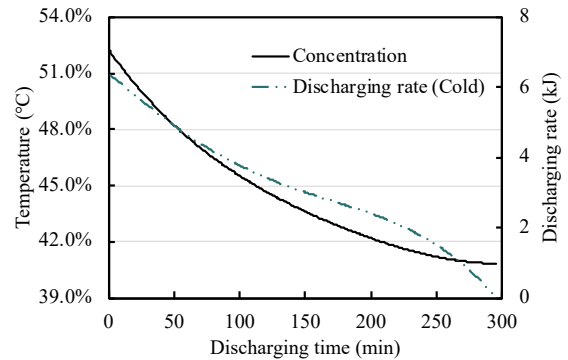


Fig. 7 Variation of the concentration and discharging rate for cooling

3.4 ESD Result

The ESD result is shown in Table 2. Generally, a larger concentration glide during discharging process leads to a larger ESD. The ESD value is comparable to the theoretical results in reference [15]. High ESD can reduce the size of the storage tanks, and also reduce the transportation cost when applied in M-TES.

Table 2. Energy storage density under different experimental conditions

Discharging	ESD _h	ESD _c	Concentration glide
Heating	580	/	41.0~52.6
Combined heating and cooling	598	534	40.2~52.8
Cooling	/	484	40.8~52.2

4. CONCLUSIONS

In this paper, a three-phase ATES test rig was established to study the dynamic characteristics and energy performance of three-phase ATES under different working conditions. Three typical working conditions are selected based on different application scenarios. Heating, cooling and combined heating and cooling are realized using the proposed three-phase ATES test rig. The ESD ranges from 484~598 (kJ/kg solution), which is much higher than most of the phase change materials. The high ESD is beneficial for its mobilized application while flexible output temperatures demonstrate its feasibility for district heating and cooling system.

ACKNOWLEDGEMENT

The authors gratefully acknowledge the support of this research by the Science and Technology Program of Guangzhou, China (201904020027).

DECLARATION OF INTEREST STATEMENT

The authors declare that they have no known competing financial interests or personal relationships that could have appeared to influence the work reported in this paper. All authors read and approved the final manuscript.

REFERENCE

[1] Raturi AK. Renewables 2019 global status report. 2019.

[2] Dai M, Li H, Wang S. Multi-agent based distributed cooperative control of air-conditioning systems for building fast demand response. *Journal of Building Engineering*. 2023;77:107463.

[3] van de Bor DM, Infante Ferreira CA, Kiss AA. Low grade waste heat recovery using heat pumps and power cycles. *Energy*. 2015;89:864-73.

[4] Du K, Calautit J, Eames P, Wu Y. A state-of-the-art review of the application of phase change materials (PCM) in Mobilized-Thermal Energy Storage (M-TES) for recovering low-temperature industrial waste heat (IWH) for distributed heat supply. *Renew Energ*. 2021;168:1040-57.

[5] Fang H, Xia J, Zhu K, Su Y, Jiang Y. Industrial waste heat utilization for low temperature district heating. *Energy Policy*. 2013;62:236-46.

[6] Zhang Y, Johansson P, Sasic Kalagasidis A. Assessment of district heating and cooling systems transition with respect to future changes in demand profiles and renewable energy supplies. *Energ Convers Manage*. 2022;268:116038.

[7] Sun F, Cheng L, Fu L, Gao J. New low temperature industrial waste heat district heating system based on natural gas fired boilers with absorption heat exchangers. *Appl Therm Eng*. 2017;125:1437-45.

[8] Guo F, Zhu X, Li P, Yang X. Low-grade industrial waste heat utilization in urban district heating: Simulation-based performance assessment of a seasonal thermal energy storage system. *Energy*. 2022;239:122345.

[9] Chardon G, Le Pierrès N, Ramousse J. On the opportunity to integrate absorption heat pumps in substations of district energy networks. *Thermal Science and Engineering Progress*. 2020;20:100666.

[10] Wang W, Guo S, Li H, Yan J, Zhao J, Li X, et al. Experimental study on the direct/indirect contact energy storage container in mobilized thermal energy system (M-TES). *Appl Energ*. 2014;119:181-9.

[11] Guo S, Zhao J, Bertrand A, Yan J. Mobilized thermal energy storage for clean heating in carbon neutrality era: A perspective on policies in China. *Energ Buildings*. 2022;277:112537.

[12] Guo S, Liu Q, Zhao J, Jin G, Wu W, Yan J, et al. Mobilized thermal energy storage: Materials, containers and economic evaluation. *Energ Convers Manage*. 2018;177:315-29.

[13] Lin Y, Xiao F, Wang S. A novel modified LiCl solution for three-phase absorption thermal energy storage and its thermal and physical properties. *International Journal of Refrigeration*. 2021;130:44-55.

[14] Wang L, Liu X, Yang Z, Gluesenkamp KR. Experimental study on a novel three-phase absorption thermal battery with high energy density applied to buildings. *Energy*. 2020;208:118311.

[15] Yu N, Wang RZ, Lu ZS, Wang LW, Ishugah TF. Evaluation of a three-phase sorption cycle for thermal energy storage. *Energy*. 2014;67:468-78.

[16] Chaudhari SK, Patil KR. Thermodynamic Properties of Aqueous Solutions of Lithium Chloride. *Physics and Chemistry of Liquids*. 2002;40(3):317-25.

[17] Conde MR. Properties of aqueous solutions of lithium and calcium chlorides: formulations for use in air conditioning equipment design. *Int J Therm Sci*. 2004;43(4):367-82.